Check for updates

ARTICLE

Clinical and genetic findings in a Chinese cohort with choroideremia

Yuning Song[1], Chunjie Chen[1], Yue Xie[1], Tengyang Sun[1], Ke Xu[1] and Yang Li[1]✉

OBJECTIVE: Choroideremia (CHM) is an X-linked chorioretinal dystrophy caused by variants in the *CHM* gene. The aim of this study was to report the clinical and genetic features of a cohort of affected males with CHM and establish the relationship between best correct visual acuity (BCVA) and age.
METHOD: Twenty-seven patients from 24 unrelated families underwent detailed ophthalmic examinations and comprehensive molecular genetic analysis. We combined the 27 patients in our own cohort with 68 Chinese patients from six previously reported studies to determine a transition age for BCVA rapid decline in 95 patients.
RESULTS: Twenty-three causal (9 novel) *CHM* variants were identified in the 27 patients, who had a mean age of 30.5 ± 17.4 years and a mean BCVA (LogMAR) of 0.61 ± 0.79. Patients at different disease stages showed different extents of retinal pigment epithelium (RPE) and choroid abnormalities. Central retinal optical coherence tomography (OCT) scanning revealed defects in the ellipsoid zone and RPE in all patients and outer retinal tubulations in 75%. The 95 patients had a mean age of 33.27 ± 16.27 years and an average (LogMAR) of 0.72 ± 0.82. The BCVA did not decline rapidly before age 25, but decreased at a mean rate of 0.037logMAR/year after that age.
CONCLUSIONS: Our results indicated Chinese patients with *CHM* variants have a younger transition age for rapid BCVA decline than previously reported for other ethnic groups. Central retinal OCT scanning can identify different abnormalities in the retinal structures, and these might be used as other parameters for monitoring disease progression in patients with CHM.

Eye (2023) 37:459–466; https://doi.org/10.1038/s41433-022-01950-6

INTRODUCTION

Choroideremia (CHM; MIM: 303100) is an X-linked chorioretinal dystrophy with a prevalence of about 1 in 100,000–50,000 [1]. It is characterized by a progressive atrophy of the choroid that coexists with loss of the retinal pigment epithelium (RPE) and photoreceptors. Male patients usually experience nyctalopia from their childhood, followed by a loss of peripheral visual field as juveniles [1, 2]. Most patients maintain a good central acuity until middle age. Full-field electroretinograms (ffERGs) initially present obvious reductions in scotopic responses, followed by decreased cone function, and cone cell death is believed to be secondary to rod cell death, as it occurs much later in the disease progression [2, 3]. Female carriers are usually asymptomatic, but signs of chorio-retinal degeneration can be detected by thorough fundus examinations. These chorio-retinal changes become relatively obvious in the second decade of life [4].

CHM is caused by variants in the *CHM* gene (MIM: 300390), which is located on chromosome Xq21.2. The *CHM* gene spans over 180 kb, consists of 15 exons, and encodes a 653 amino acid protein, Rab Escort Protein 1 (REP1) [1–3]. The ubiquitously expressed REP1 is involved in intracellular trafficking of vesicles and post-translational modification of Rab proteins [5]. At present, over 380 disease-causing variants in the *CHM* gene have been reported. Most of them are loss-of-function variants that abolish functional REP-1, whereas missense variants are uncommon [2, 3]. Previous studies have not established any clear genotype–phenotype correlation [2, 3, 6].

Two recent studies reported the encouraging results of human I/II clinical trials for the retinal gene therapy of CHM [7, 8]. Therefore, knowing the rate of disease progression is essential for establishing a practical time window for future retinal gene therapy. Some previous studies and a very recent study have suggested that the decline in best corrected visual acuity (BCVA) of patients with CHM follows a two-phase linear model (a slow decline phase followed by a rapid decline phase), with an estimated transition age between 30 and 60 years [9–12]. In contrast, the results of a very recent study cohort that included 48 Chinese affected males with CHM indicated that the defect of visual acuity was more serious in the Chinese population than in the western population [13]. The transition age for the Chinese patients was approximately 20 years, which is much younger than the ages observed in western patients [13].

Comprehensive studies of the clinical and genetic features of patients with CHM have been conducted in the western population, but similar studies are lacking in Chinese patients. In the current study, we characterized the phenotypes and genotypes of 27 Chinese male patients and then combined our cohort of

[1]Beijing Institute of Ophthalmology, Beijing Tongren Eye Center, Beijing Tongren Hospital, Beijing Ophthalmology & Visual Sciences Key Lab, Capital Medical University, Beijing, China. ✉email: yanglibio@aliyun.com

27 patients with 68 Chinese patients from 6 previously published studies [13–18] to estimate a transition age of the decline of BCVA in Chinese patients with CHM.

SUBJECTS AND METHODS

Patients
We performed this retrospective study according to the tenets of the Declaration of Helsinki for research relating to human subjects. All molecular analysis methods were prospectively evaluated and permitted by the ethics committee of Beijing Tongren Hospital. In this study, 27 male patients clinically diagnosed with CHM or retinitis pigmentosa (RP) from 24 unrelated families were recruited from Beijing Tongren Hospital from 2004 to 2020. Three of the 24 families had two patients. Their diagnosis was further confirmed by identification of a disease-causing variant of the CHM gene by the Genetics Laboratory of the Beijing Institute of Ophthalmology. Each participant underwent clinical examinations, including best-corrected visual acuity (BCVA) using E decimal charts, slit-lamp biomicroscopy, and fundus examination and photography. Nineteen patients had full-field electroretinogram (ERG) examination, 19 participants underwent fundus autofluorescence (FAF) evaluation, and 14 patients had visual field testing. Twenty patients (40 eyes) underwent central retinal optical coherence tomography (OCT) scanning using a Spectralis OCT instrument (Heidelberg Engineering, Germany) to obtain high-speed vertical and horizontal single-line scanning images (8.9 mm × 8.9 mm through the macula). Numeric averages of retinal thicknesses and volumes were obtained from a thickness map established by the Early Treatment Diabetic Retinopathy (EDTRS) grid using Heidelberg software (Heidelberg Engineering). The average thickness of all points within the inner 1 mm circle centered at the fovea are defined as the central subfield thickness (CST).

The patients were classified into three stages based on their fundus appearance, according to a fundoscopic classification described by Krill [19]. In stage 1, the patients showed pigmentary changes with or without a demarcated scalloped-like atrophy of the choroid and RPE in the peripheral or midperipheral fundus. In stage 2, patients presented with atrophy of the choroid and RPE from the equatorial regions inward and from the optic disc outward, with small islands of the central retina preserved in the posterior region. In stage 3, patients displayed extensive widespread chorioretinal atrophy, resulting in a whitish fundus appearance (Fig. 1).

PCR-based sequencing of the CHM gene
After informed consent was obtained, peripheral blood samples were collected from all patients and their available family members, and genomic DNA was extracted from peripheral blood leukocytes using a genomic DNA extraction kit (Vigorous, Beijing, China), according to the manufacturer's protocol. Fifteen exons and flanking splicing sites of the CHM gene were amplified by PCR in 21 probands. The PCR amplifications were done using regular reaction mixtures, and purified amplicons were directly sequenced on an ABI Prism 373A DNA sequencer (Applied Biosystems, Foster City, CA). The sequencing results were compared with a standard DNA sequence of CHM (GenBank NM_000390). For the CHM gene, cDNA numbering + 1 refers to A in the initiation AUG translation codon in CHM.

Targeted exome sequencing
We performed targeted exome sequencing (TES) in seven patients who were initially diagnosed with RP or whose Sanger sequencing of the CHM gene was normal, using a capture panel previously developed and evaluated by our group [20]. The capture panel consisted of 188 known inherited retinal degeneration genes. The Illumina library preparation and capture experiment were performed as previously [20].

Bioinformatics analysis
Two databases, the HGMD database (http://www.hgmd.cf.ac.uk/ac/index.php) and the LOVD database (https://grenada.lumc.nl/LOVD2/eye/home.php), were used to search for reported pathogenic variants. The pathogenicity of the variants was predicted by three in silico programs: PolyPhen2 (http://genetics.bwh.harvard.edu/pph, in the public domain), Mutation Taster (http://www.mutationtaster.org, in the public domain), and SIFT (http://sift.jcvi.org/, in the public domain). The programs NetGene2 Server (http://www.cbs.dtu.dk/services/NetGene2/),
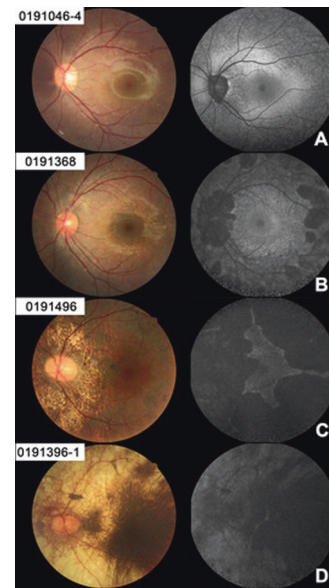

Fig. 1 Colored fundus (CF) and fundus autofluorescence (FAF) photographs of patients with CHM at different stages. A, B CF and FAF images of patients 0191046-4 and 0191348 at stage 1 show pigmentary changes in the midperipheral fundus or with a couple of demarcated scallop-like atrophies of the choroid and RPE in the peripheral or midperipheral retina. **C** CF and FAF photographs of patient 0191496 at stage 2 show a spread of the choroidal atrophy from the equatorial regions inward and from the optic disc outward, leaving an irregular central island on the posterior pole. **D** CF and FAF images of patient 0191396-1 at stage 3 display extensive and widespread chorioretinal atrophy, resulting in a typical whitish fundus appearance due to the illumination of the exposed sclera.

Human Splice Finder (HSF, http://www.umd.be/HSF3/), and Berkeley Drosophila Genome Project (BDGP, http://www.fruitfly.org/seq_tools/splice.html) were used to analyze any variants involving a splicing effect. Co-segregation analysis was performed whenever DNA of any family members was available.

Copy number variation (CNV) analysis and validation
The CNV kit software (https://github.com/etal/cnvkit) was used to detect CNVs from variations in the read depth for the patients having TES data [21]. Real-time q-PCR was subsequently performed to verify the presence of the assumed CNVs of CHM in five families, as we described earlier [22].

Statistical analysis
We combined the 27 patients in our current cohort with 68 Chinese male patients from six previously reported studies [13–18] to determine a transition age for BCVA rapid decline in the Chinese population. These six studies described the age, BCVA, and variants of the CHM of 68 patients from 54 unrelated families (Table S1). We converted the Snellen ratios into the logarithm of the minimum angle of resolution (logMAR) values for statistical purposes. The logMAR values of 0, 1.0, 1.85, 2.3, and 2.7 are equal to a Snellen vision of 1.0, 0.1, counting fingers, hand movements, and light perception, respectively. We obtained a range of cutoff points for the two-phase model of vision decreases with age by establishing a prediction model. Linear, exponential, power, quadratic, and cubic functions were used to fit the data. For the age range (15–30 years), the segmented linear regression analysis was carried out using a preset integer age until the maximum R^2 of the segmented linear trend was achieved. Statistical significance was defined as $P < 0.05$. The results of other studies were compared using the better-seeing eyes. Binocular symmetry was determined by correlation coefficients. Kaplan–Meier survival analyses of BCVA as a function of age were performed with three endpoints: <0 (logMAR, equal 85 letters), <0.3 (logMAR, equal 70 letters), and <1.0 (logMAR, equal 35 letters). Kaplan–Meier survival analysis was also performed for the right, the left, and the better-seeing eyes.

RESULTS

CHM variants

We detected 22 distinct disease-causing variants of *CHM* in the 24 unrelated families. The variants included nine nonsense variants, six frameshifts indels, three splicing effects, three CNVs, and one variant in the promoter region. Only one large deletion, encompassing exons 1 to 15, was identified in three unrelated families; the remaining 21 variants were detected in one family. Of the 22 variants, nine were first found in the current cohort. These nine novel variants comprised three nonsense variants, three frameshift small indels, one splice effect, one large duplication, and one variant in the promoter region. None of these novel variants were previously recorded in any public database, and all were defined as pathogenic or likely pathogenic based on the American College of Medical Genetics and Genomics (ACMG) guidelines and standards (Table 1).

Clinical findings

Except for one 9-year-old proband (010275), the patients from the 24 unrelated families in the current study all first experienced night blindness, followed by different extents of defects in visual acuity (in 80% of the patients, 21/27). Their mean age at onset of nyctalopia was 10.3 ± 8.8 years (range 3–40). Two probands (019524 and 019737) also complained of mild hearing loss. The main clinical characteristics of each patient are summarized in Table 2.

The relationship between age and visual acuity

The mean age at the last examination for the 27 patients was 30.5 ± 17.4 years (range 6–67). According to Krill's classification, these patients included five patients in stage 1, 11 patients in stage 2, and 11 patients in stage 3. The mean age for the establishment of stage 1 (9.40 ± 2.73 years, range 6–13) and stage 2 (22.09 ± 5.20 years, range 14–28) was significantly younger than for stage 3 (48.55 ± 10.75 years, range 34–67) ($p < 0.001$ and $p = 0.003$, respectively). The mean BCVA (LogMAR) of the 27 patients at the last time of examination was 0.61 ± 0.79 (range 0–2.70). The mean BCVA for the patients in stage 1 (0.17 ± 0.27, range 0–0.70) and stage 2 (0.27 ± 0.32, range 0–1.10) was significantly better than for the patients in stage 3 (1.16 ± 0.94, ranger 1.10–2.7) ($p < 0.001$ and $p = 0.002$).

We obtained a more precise relationship between BCVA and age of Chinese patients with CHM by combining the 27 patients in the current cohort with 68 Chinese patients from six previously published studies [13–18]. The mean age of the 95 patients was 33.27 ± 16.27 years (range 5–78), and their average (LogMAR) was 0.72 ± 0.82 (range 0–2.70). The fitting models for BCVA of the better-seeing eyes and age in the 95 patients showed that the quadratic function gave the best fit ($R^2 = 0.5532$; $p < 0.001$; $Y = 0.4361 + 0.02320X + 0.0005193 \times^2$) (Fig. 2A). For the shape characteristics of the quadratic function, we selected a cutoff point range from age 15 to 30 years. In this range, we found that segmented linear regression at intervals of one year gave the highest R^2 for an estimated age of 25 years. No significant correlation was detected between BCVA (LogMAR) and age in patients $\leq$ 25 years ($R^2 = 0.1951$; $p = 0.0759$; $Y = 0.01589X - 0.01825$); however, a significant positive correlation was observed between BCVA (LogMAR) and age in patients over 25 years of age ($R^2 = 0.4318$; $p < 0.0001$; $Y = 0.03711X - 0.8694$). For the patients older than 25 years, the rate of decline in their logMAR BCVA was 0.037 units per year (ERDTS score was 1.85 letters/year).

We also evaluated the binocular symmetry of BCVA in the 95 patients and found a strong correlation coefficient for BCVA ($R = 0.7584$; $p < 0.0001$)(Fig. 2B). Kaplan–Meier survival analysis performed to display the age distribution for visual acuity decline revealed that the survival plots for the right, left, and the better-seeing eyes showed substantial overlap and that the calculated median age when the BCVA decreases above 0 (logMAR) was 34 years. The calculated median age when the BCVA dropped above 0.3 (logMAR) was 44 and 46 years for both eyes and the better-seeing eyes, respectively. The calculated median age when the BCVA was above 1.0 (logMAR) was 63, 53, and 63 years for the right, left, and better-seeing eyes, respectively.

Fundus features

Of the five patients (ten eyes) in stage 1, two patients showed only pigmentary changes in the midperipheral fundus, while the other three patients also presented with spots of demarcated scalloped-like atrophy of the choroid and RPE in the peripheral or midperipheral retina (Fig. 1A, B). Their FAF displayed either a mottled hypo- or hyper-autofluorescence (AF) (Fig. 1A), along with several demarcated scalloped hypo-AF regions (Fig. 1B). The 11 patients in stage 2 presented with extensive atrophy of the RPE and choroid toward the central retina, leaving an irregular central island on the posterior pole (Fig. 1C). Scattered bone spicules were observed in the peripheral or midperipheral retina or around the optic disc. The FAF showed a hyper-AF region corresponding to the central island with a large area of hypo-AF in the remaining retina. (Fig. 1C). The 11 patients in stage 3 displayed extensive and widespread chorioretinal atrophy, resulting in a typical whitish fundus appearance due to the illumination of the exposed sclera (Fig. 1D). Their FAF showed an entire hypo-AF retina with a very tiny hyper-AF region in the macula (Fig. 1D).

Central retinal structural features evaluated by SD-OCT

We performed SD-OCT scanning in 20 patients (40 eyes) in the current cohort, including five patients in stage 1, eight patients in stage 2, and seven patients in stage 3. For the five patients in stage 1, SD-OCT examination revealed a normal central retinal architecture, including the macula, but disruption or defects of the ellipsoid zone (EZ) and RPE in the paramacular region (Fig. 3A, B). The mean central subfield thickness (CST) was 218.88 ± 14.72 μm (range 196–241). No outer retinal tubulations (ORTs) or cystoid cavities were observed in the ten eyes, except for the left eye of Proband 0191368, which showed a very tiny cystoid space in the inner nuclear layer (Fig. 3B). For the 8 patients in stage 2, OCT revealed an almost normal macular architecture in 15 eyes and macular disorganization in only one eye. The mean CST was 232.79 ± 21.94 μm (range 185–257). Defects were observed in the EZ and RPE in the macular regions in all 16 eyes. In addition, ORTs and atrophy of the outer retina, RPE, and choroid were observed in the para-macular region in all 16 eyes (Fig. 3C–F). Small cystoid cavities in the inner retina, suggestive of a schisis, were observed in 14 eyes. For the seven patients in stage 3, OCT examination revealed atrophy of the entire retina, RPE, and choroid. ORTs and small cystoid cavities were observed in all 14 eyes (Fig. 3G, H). The mean CST was 137.6 ± 55.13 μm (range 55–218), which was significantly thinner than the CST observed in stage 1 and 2 patients ($p = 0.04$ and $p < 0.001$). An epiretinal membrane was observed in 7 patients (14 eyes) who were in stage 2 or 3 (Table 2).

Full-field electroretinography

In the current cohort, 19 patients underwent ERG recording. Three patients in stage 1 and 4 patients in stage 2 showed severe dysfunction of cones and rods or absent rod function with moderate or severe cone dysfunction, while six patients in stage 2 and three patients in stage 3 presented with an extinguished recording.

DISCUSSION

The current study depicts the clinical and genetic findings of 27 male patients from 24 unrelated families with molecularly confirmed CHM. We established a relatively accurate association between BCVA and age in 95 Chinese male patients with CHM (27 patients in the current cohort and 68 patients from six

Table 1. Presumed pathogenic *CHM* variants identified in this study and analysis of the variants by predictive programs.

Exon/ intron	Nucleotide change	Protein effect	Allele frequency	MT	SIFT	PP-2	Net-Gene2	BDGP	ASSP	ExAC	1000 G	MAF	ACMG	Source
1	c.-98C>G	–	1	–	–	–	–	–	–	–	–	–	LP	Novel
4	c.282_283insT	p.I95Yfs*16	1	DC	–	–	–	–	–	–	–	–	PA	Novel
5	c.315_318delTCAG	p.S105Rfs*20	1	DC	–	–	–	–	–	–	–	–	PA	[28]
5	c.638delA	p.N213Tfs*19	1	DC	–	–	–	–	–	–	–	–	PA	Novel
5	c.651 C>G	p.Y217X	1	DC	–	–	–	–	–	–	–	–	PA	Novel
5	c.653 C>A	p.S218X	1	DC	–	–	–	–	–	–	–	–	PA	Novel
6	c.715 C>T	p.R239X	1	DC	–	–	–	–	–	1E−05	–	–	PA	[10]
6	c.808 C>T	p.R270X	1	DC	–	–	–	–	–	–	–	–	PA	[10]
6	c.820-1 G>T	–	1	DC	–	–	SC	SC	SC	–	–	–	PA	[23]
6	c.820-2 A>G	–	1	DC	–	–	SC	SC	SC	–	–	–	PA	[11]
7	c.877 C>T	p.R293X	1	DC	–	–	–	–	–	–	–	–	PA	[13]
8	c.1153delC	p.Q385Sfs*23	1	DC	–	–	–	–	–	–	–	–	PA	[13]
8	c.1153 C>T	p.Q385X	1	DC	–	–	–	–	–	–	–	–	PA	Novel
10	c.1342 C>T	p.Q448X	1	DC	–	–	–	–	–	–	–	–	PA	LOVD database
10	c.1327_1328delAT	p.M443Vfs*18	1	DC	–	–	–	–	–	–	–	–	PA	[10]
11	c.1383_1384insGA	p.S462Afs*4	1	DC	–	–	–	–	–	–	–	–	PA	Novel
11	c.1414-1 G>A	–	1	DC	–	–	SC	SC	SC	–	–	–	PA	Novel
14	c.1618C>T	p.Q540X	1	DC	–	–	–	–	–	–	–	–	PA	[30]
14	c.1695delT	p.Y565X	1	DC	–	–	–	–	–	–	–	–	PA	[25]
1-15	Exon1-15 del	–	3	–	–	–	–	–	–	–	–	–	PA	[13]
1-2	Exon 1-2 del	–	1	–	–	–	–	–	–	–	–	–	PA	[31]
5-12	Exon5-12 dup	–	1	–	–	–	–	–	–	–	–	–	PA	Novel

Abbreviations: ACMG classification of variants according to American College of Medical Genetics; MAF Minor Allele Frequency; DC Disease causing; SC Splice site changed; MAF Minor Allele Frequency; PA Pathogenic; LP Likely pathogenic; US uncertain Significance.

Table 2. Clinical features and results of the *CHM* gene variants screening of the male patients.

Patient ID	Age (year) exam	Onset	BCVA(OD/OS) Decimal Acuity	LogMAR	Nyctalopia	Fundus*	OCT Findings (OD/OS, OU) ORTs	Cyst cavity	Epiretinal membrane	ERG	Variants	Co-segregation
010275	9	4	0.50/0.50	0.70/0.70	NO	1	NO	NO	NO	Rod Ex,cone SD	Exon1_15 del	NA
019015	28	5	0.80/0.40	0.10/0.40	YES	2	NA	NA	NA	Ex	c.1414-1 G > A	NA
019107	24	24	0.80/0.80	0.10/0.10	YES	2	NA	NA	NA	NA	Exon1_15 del	NA
019146	34	7	0.60/0.60	0.22/0.22	YES	3	NA	NA	NA	Ex	pQ448*	NA
019240	59	29	0.50/0.70	0.30/0.15	YES	3	NA	NA	NA	Ex	pR293*	NA
019271	36	4	0.60/0.70	0.22/0.15	YES	3	NA	NA	NA	NA	pI95Yfs*16	NA
019330	14	5	0.08/0.08	1.10/1.10	YES	2	NA	NA	NA	Ex	pN213Tfs*1	NA
019348	22	15	1.00/1.00	0.00/0.00	YES	2	YES	NO	NA	SD	pS218*	YES
019524	46	5	0.20/0.05	0.70/1.30	YES	3	NA	NA	NA	NA	pR270*	NA
019637	49	5	0.20/HM	0.70/2.30	YES	3	YES	NO	NO	NA	pY217*	NA
019737	50	20	0.5/LP	0.30/2.70	YES	3	YES	NFL	YES	Ex	pS105Rfs*20	NA
019820	28	16	1.00/0.80	0.00/0.10	YES	2	YES	IN	NO	Ex	pM443Vfs*18	NA
019941	23	4	0.70/0.40	0.15/0.40	YES	2	YES	IN	YES	Ex	pQ385*	NO
019993	26	14	0.50/0.50	0.30/0.30	YES	2	YES	IN	YES	SD	c.820-2 A > G	YES
0191045	16	10	0.90/0.90	0.05/0.05	YES	2	YES	NO	NO	SD	pY565*	YES
0191046	41	12	HM/HM	2.30/2.30	YES	3	YES	IN,ON	YES	Ex	Exon1_2 del	YES
0191046-4	13	5	1.00/1.00	0.00/0.00	YES	1	NO	NO	NO	NA	Exon1_2 del	YES
0191240	14	7	0.50/0.60	0.30/0.22	YES	2	YES	IN	NO	Ex	pR239*	YES
0191247	36	3	0.80/0.80	0.10/0.10	YES	3	YES	ON	NO	Ex	pS462Afs*4	YES
0191273	6	4	1.00/0.80	0.00/0.10	YES	1	NO	NO	NO	Rod Ex, cone MD	pQ385Sfs*23	YES
0191368	12	11	0.80/1.00	0.10/0.00	YES	1	NO	NO/IN#	NO	SD	c.820-1 G > T	YES
0191368-2	67	5	FC/HM	1.85/2.30	YES	3	YES	IN	YES	NA	c.820-1 G > T	YES
0191396	7	6	1.00/0.80	0.00/0.10	YES	1	NO	NO	NO	NA	pQ540*	YES
0191396-1	53	5	0.05/0.05	1.30/1.30	YES	3	YES	IN,IP	YES	NA	pQ540*	YES
0191496	28	5	1.00/1.00	0.00/0.00	YES	2	YES	IN	NO	Rod Ex, cone SD	c.-98C > G	YES
0191524	63	40	HM/HM	2.30/2.30	YES	3	YES	ON	YES	Ex	Exon1_15 del	NA
0191531	20	7	0.30/0.20	0.52/0.70	YES	2	YES	NFL	NO	Ex	Exon5_12 dup	YES

Abbreviations: BCVA best-corrected visual acuity; FC finger counting; HM hand move; NA data not available; SD severe damage; NE Not exist; E exist *Classification according to Krill and Berger: 1 = abNErmal pigmentary stripping and fine atrophy of the retinal pigment epithelium, mild atrophy of the larger choroidal vessels and focal areas of choriocapillary atrophy, 2 = spread of the choroidal atrophy from the equatorial regions inward and from the optic disc outward, 3 = widespread chorioretinal atrophy, attenuation of retinal vessels, and mild optic disc pallor.
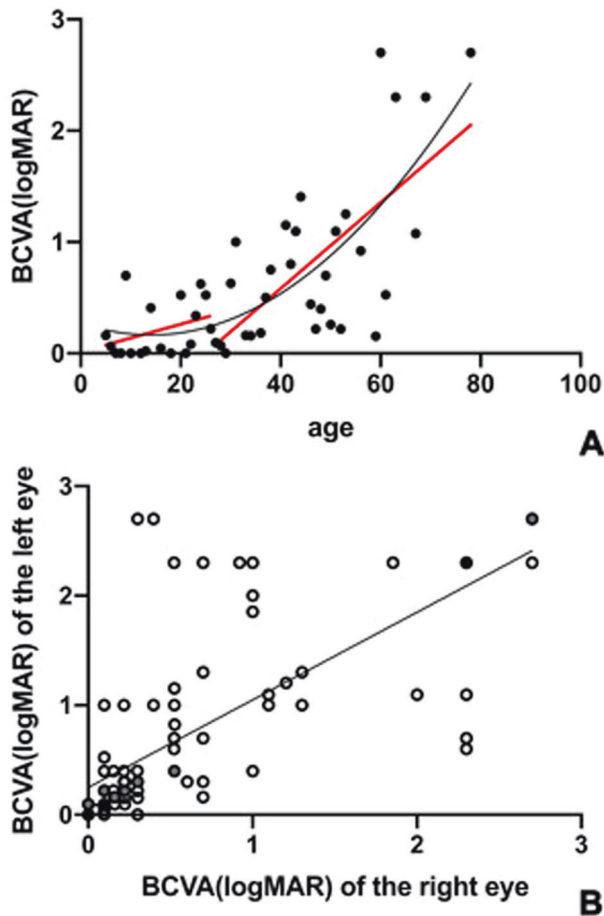
Fig. 2 Best-corrected visual acuity (BCVA) as a function of age in the 95 better-seeing eyes of 95 patients with CHM. A BCVA as a function of age in the 95 better-seeing eyes of 95 patients with CHM, including the 27 patients in our cohort and 68 patients from six previously published Chinese studies. The black line is the quadratic function of the best fit. The red line shows that the sample population is divided at a critical age (25 years old) into a ≤ 25 year age group and a > 26 year age group. Each point is the average after processing duplicate values. **B** Symmetry between the BCVA of the right and left eyes with choroideremia. A moderate correlation was detected between the BCVA of the right and left eyes (R2 = 0.5751; $P < 0.0001$).

previously published studies), and we determined the transition age for rapid decline of visual acuity and progression rate. We also confirmed the highly binocular symmetry in BCVA in this large Chinese cohort.

All disease-causing variants identified in the current cohort were obvious loss-of-function variants, but a novel variant c.-98C > G was located in the non-coding region of the *CHM*. The position c.-98C is situated in the promoter region (c.-119 to c.-76) and the base C in the position c.-98 is highly conserved among mammals [2]. Two previously reported variants at the same position (c.-98: C > A and C > T) completely abolished luciferase activity when introduced into a reporter construct [23], suggesting a loss-of-function effect. As the variant c.-98C > G was not recorded in any public databases and co-segregated with the phenotype, we defined it as likely pathogenic based on the ACMG standard.

Visual acuity is considered a pivotal factor for following patients with CHM. Since Coussa et al. [24] first proposed a two-phase linear model for the decrease in BCVA in eyes with CHM, several studies have used this model to explore the transition age as a cutoff point that initiates the rapid visual loss phase; however, the

cutoff points of the two phases obtained from different studies varied from 30 to 60 years of age [9, 10, 24, 25]. A very recent meta-analysis study, which included 1004 eyes in 693 affected males, reported that the decline in BCVA actually followed a two-phase linear model with a transition age of 39.1 years [12]. The rate of decline of BCVA was estimated at 1.23 letters/year (equivalent to 0.025logMAR/year) after 39 years. Another study that included 48 Chinese patients revealed a transition age of 20 years for Chinese patients with CHM, which was much younger than the transition age observed in western patients [13]. Considering the small numbers of Chinese patients in our cohort, we combined our patients with the 68 Chinese patients described in six previous studies [13–18] and calculated a transition age using the method of function fitting combined with preset piecewise regression. Our results showed a transition age of 25 years, which was relatively close to the age of 30 years described by Heon et al. [25], but much younger than the ages described in several Caucasian studies [9, 10, 12, 24] and a transition age of 40 years recently reported in Japanese patients [26]. The estimated rate for the decline in BCVA after the age of 25 years was 0.037logMAR/year, which was between 0.025–0.048 logMAR/year [10–12, 27].

Consistent with the younger transition age, our Kaplan–Meier survival analysis revealed that the estimated median ages (34 and 63 years) when the BCVA was above 0 and 1.0 (logMAR) for the better-seeing eye were also younger than the ages (47 and 72 years) described by Han et al. [12]. They also found that the transition age was widely scattered and that some patients experienced a rapid decline in BCVA at a young age [12]. Classification of our 27 patients into three stages according to the previous fundus image classification standards [19] revealed much younger mean ages (9.4 and 22.1 years) for patients in stages 1 and 2 than were reported for the median ages (30.7 and 33.6 years) described by Di Iorio et al., who classified their 51 patients using the same method [11]. Consistent with the findings in Caucasian patients, over 90% of the patients in the large cohort carried a null variant of *CHM*, we deduced that the young transition-age observed in Chinese patients might be due to genetic modifiers or environmental factors such as dietary structure etc.

We identified disruption or defects in the ellipsoid zone (EZ) and RPE at the central retina in all patients as early as age six using OCT scanning. Heon et al. previously reported that the central retinal thickness was significantly correlated with BCVA and the age of the patients with CHM [25]. Our results also revealed that the BCVA of patients in stages 1 and 2, who had a relatively normal architecture in the macular region and a normal central retinal thickness, was significantly better than the BCVA of the patients in stage 3, who had obvious retinal atrophy in the macula. ORTs have been detected in other inherited retinal diseases and are especially frequent in Bietti crystalline dystrophy [28]. We found ORTs in all our stage 2 and 3 patients, but not in the patients in stage 1. We noticed that ORTs were usually located between the relatively normal and the atrophied regions of the outer neural retina and were closer to the fovea as the disease progressed, consistent with observations described in previous studies [27, 29]. The ORTs in CHM are considered a consequence of an unusual form of retinal remodeling [25, 29]. We detected epiretinal membrane in the macula in seven patients (35%, 7/20), including two patients in stage 2 and five patients in stage 3, suggesting that its presence indicated advanced-stage, rather than early-stage, disease. Therefore, changes in the central retinal structures might be used as other parameters for monitoring the disease progression in patients with CHM.

The current study has several limitations. One is its retrospective design and another is that the number of patients in our own cohort is relatively small. We also did not conduct any quantitative analysis for OCT and FAF, so we cannot accurately describe the characteristics of the changes in the patient images.
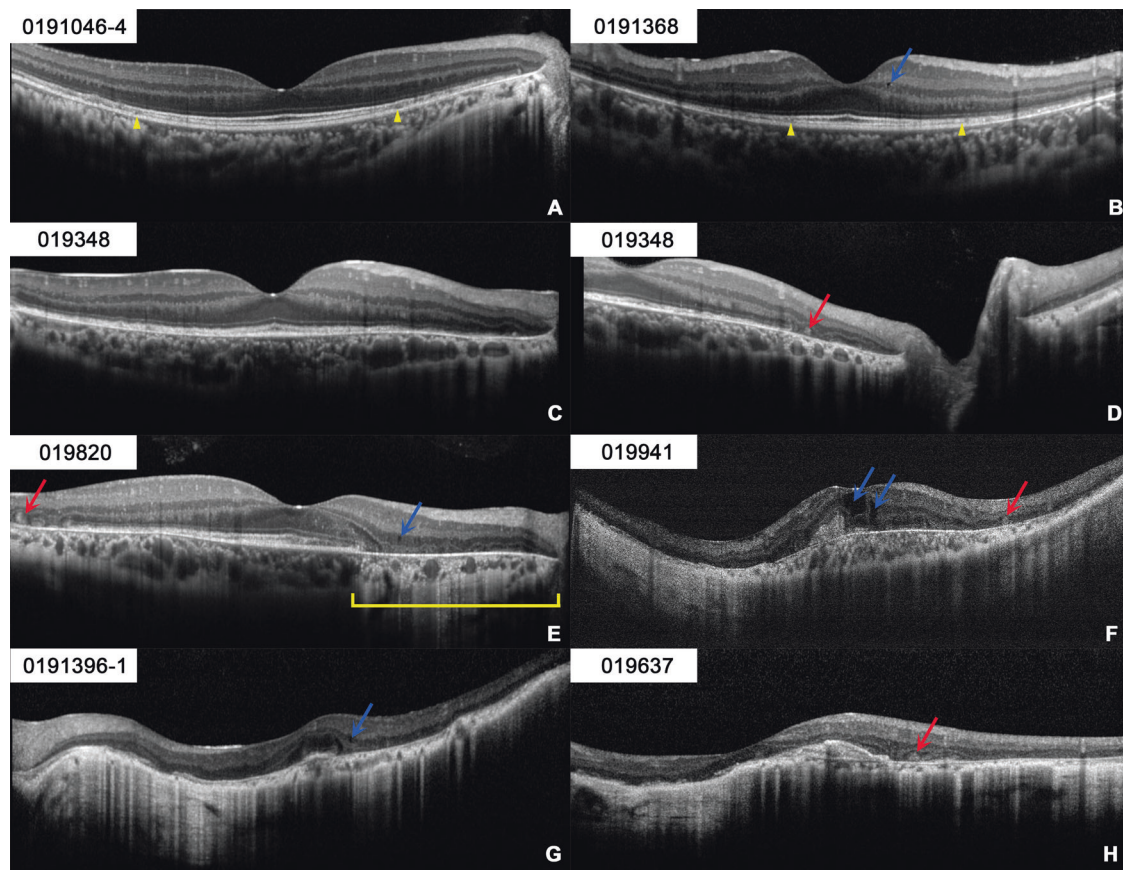
Fig. 3 Central retinal OCT images of patients with CHM at the different stages. A, **B** OCT scans of patients 0191046-4 (13 y) and 0191368 (12 y) in stage 1 show the normal central retinal architecture, but disruption or defects of the EZ and RPE in the paramacular region. **C–F** OCT scans of patients 019348 (22 y), 019820 (28 y), and 019941(23 y) in stage 2 present the defects in the EZ and RPE, outer retinal tubulations (ORTs), small cystoid cavities, and atrophy of the outer retina, RPE, and choroid in the central retina. **G**, **H** OCT scans of patients 0191396-1 (53 y) and 019637 (49 y) in stage 3 display atrophy of the entire retina, RPE, and choroid, small cystoid cavities in the inner nuclear layer, and ORTs. The red arrows indicate outer retinal tubulations (ORTs). The blue arrows designate cystoid cavities. Yellow triangles show starting points of defects of the ellipsoid zone (EZ) and RPE in the paramacular region. Yellow line designated atrophy of the outer retina, RPE, and choroid in the para-macular region.

In conclusion, our results indicate that Chinese patients with *CHM* variants have a younger transition age for rapid BCVA decline than previously reported for other ethnic groups and that Chinese patients tend to have more severe CHM-related visual defects. Central retinal OCT scanning can identify different abnormalities in the retinal structures, and these might be used as other objective parameters for monitoring disease progression in patients with CHM.

Summary
What was known before

- The decline in best-corrected visual acuity (BCVA) of patients with CHM follows a two-phase linear model, with an estimated transition age between 30 and 60 years

What this study adds

- Chinese patients with CHM variants have a younger transition age for rapid BCVA decline than previously reported for other ethnic groups.
- Central retinal OCT scanning can identify different abnormalities in the retinal structures, and these might be used as other parameters for monitoring disease progression in patients with CHM.

REFERENCES

1. Moosajee M, Ramsden SC, Black GC, Seabra MC, Webster AR, Clinical utility gene card for: choroideremia. Eur J Hum Genet. 2014; 22.
2. Dimopoulos IS, Radziwon A, St Laurent CD, MacDonald IM. Choroideremia. Curr Opin Ophthalmol. 2017;28:410–5.
3. Dimopoulos IS, Chan S, MacLaren RE, MacDonald IM. Pathogenic mechanisms and the prospect of gene therapy for choroideremia. Expert Opin Orphan Drugs. 2015;3:787–98.
4. Murro V, Mucciolo DP, Passerini I, Palchetti S, Sodi A, Virgili G, et al. Retinal dystrophy and subretinal drusenoid deposits in female choroideremia carriers. Graefes Arch Clin Exp Ophthalmol. 2017;255:2099–111.
5. Corbeel L, Freson K. Rab proteins and Rab-associated proteins: major actors in the mechanism of protein-trafficking disorders. Eur J Pediatr. 2008; 167:723–9.
6. Simunovic MP, Jolly JK, Xue K, Edwards TL, Groppe M, Downes SM, et al. The spectrum of CHM gene mutations in choroideremia and their relationship to clinical phenotype. Invest Ophthalmol Vis Sci. 2016;57:6033–9.
7. Pennesi ME, Birch DG, Duncan JL, Bennett J, Girach A. Choroideremia: retinal degeneration with an unmet need. Retina. 2019;39:2059–69.
8. Lam BL, Davis JL, Gregori NZ, MacLaren RE, Girach A, Verriotto JD, et al. Choroideremia gene therapy phase 2 clinical trial: 24-month results. Am J Ophthalmol. 2019;197:65–73.
9. Roberts MF, Fishman GA, Roberts DK, Heckenlively JR, Weleber RG, Anderson RJ, et al. Retrospective, longitudinal, and cross sectional study of visual acuity impairment in choroideraemia. Br J Ophthalmol. 2002;86:658–62.
10. Freund PR, Sergeev YV, MacDonald IM. Analysis of a large choroideremia dataset does not suggest a preference for inclusion of certain genotypes in future trials of gene therapy. Mol Genet Genom Med. 2016;4:344–58.

11. Di Iorio V, Esposito G, De Falco F, Boccia R, Fioretti T, Colucci R, et al. CHM/REP1 transcript expression and loss of visual function in patients affected by choroideremia. Invest Ophthalmol Vis Sci. 2019;60:1547–55.

12. Shen LL, Ahluwalia A, Sun M, Young BK, Grossetta Nardini HK, Del Priore LV. Long-term natural history of visual acuity in eyes with choroideremia: a systematic review and meta-analysis of data from 1004 individual eyes. Br J Ophthalmol. 2020;105:271–8.

13. Han X, Wu S, Li H, Zhu T, Wei X, Zhou Q, et al. Cincal charateristic and melecualr genetic analyis of a cohort of Chinese patients with choroideremia. Retina. 2020;40:2240–53.

14. Cai XB, Huang XF, Tong Y, Lu QK, Jin ZB. Novel CHM mutations identified in Chinese families with Choroideremia. Sci Rep. 2016;6:35360.

15. Guo H, Li J, Gao F, Li J, Wu X, Liu Q. Whole-exome sequencing reveals a novel CHM gene mutation in a family with choroideremia initially diagnosed as retinitis pigmentosa. BMC Ophthalmol. 2015;15:85.

16. Lin Y, Liu X, Luo L, Qu B, Jiang S, Yang H, et al. Molecular analysis of the choroideremia gene related clinical findings in two families with choroideremia. Mol Vis. 2011;17:2564–9.

17. Gao FJ, Tian GH, Hu FY, Wang DD, Li JK, Chang Q, et al. Next-generation sequencing-based clinical diagnosis of choroideremia and comprehensive mutational and clinical analyses. BMC Ophthalmol. 2020;20:212.

18. Dan H, Li T, Lei X, Huang X, Xing Y, Shen Y. Whole exome sequencing of a family revealed a novel variant in the CHM gene, c.22delG p.(Glu8Serfs*4), which co-segregated with choroideremia. Biosci Rep. 2020;40:BSR20200067.

19. Krill AE, Hereditary retinal and choroidal diseases. Harper & Row Press: Hagerstown, USA, 1972.

20. Sun T, Xu K, Ren Y, Xie Y, Zhang X, Tian L, et al. Comprehensive molecular screening in chinese usher syndrome patients. Invest Ophthalmol Vis Sci. 2018;59:1229–37.

21. Talevich E, Shain AH, Botton T, Bastian BC. CNVkit: genome-wide copy number detection and visualization from targeted DNA sequencing. PLoS Comp Biol. 2016;12:e1004873.

22. Dong B, Chen J, Zhang X, Pan Z, Bai F, Li Y. Two novel PRP31 premessenger ribonucleic acid processing factor 31 homolog mutations including a complex insertion-deletion identified in Chinese families with retinitis pigmentosa. Mol Vis. 2013;19:2426–35.

23. Radziwon A, Arno G, D KW, McDonagh EM, Baple EL, Webb-Jones K, et al. Single-base substitutions in the CHM promoter as a cause of choroideremia. Hum Mutat. 2017;38:704–15.

24. Coussa RG, Kim J, Traboulsi EI. Choroideremia: effect of age on visual acuity in patients and female carriers. Ophthalmic Genet. 2012;33:66–73.

25. Heon E, Alabduljalil T, McGuigan DB III, Cideciyan AV, Li S, Chen S, et al. Visual function and central retinal structure in choroideremia. Invest Ophthalmol Vis Sci. 2016;57:OCT377–387.

26. Hayashi T, Kameya S, Mizobuchi K, Kubota D, Kikuchi S, Yoshitake K, et al. Genetic defects of CHM and visual acuity outcome in 24 choroideremia patients from 16 Japanese families. Sci Rep. 2020;10:15883.

27. van Schuppen SM, Talib M, Bergen AA, Ten Brink JB, Florijn RJ, Boon CJF, et al. Long-term follow-up of patients with choroideremia with scleral pits and tunnels as a novel observation. Retina. 2018;38:1713–24.

28. Li Q, Li Y, Zhang X, Xu Z, Zhu X, Ma K, et al. Utilization of fundus autofluresence, spectral domain optical coherence tomography, and enhanced depth images in the charaterization of Bietti crystalline dystrophy in different stages. Retina. 2015;35:2074–84.

29. Khan KN, Islam F, Moore AT, Michaelides M. Clinical and genetic features of choroideremia in childhood. Ophthalmology. 2016;123:2158–65.

30. Ramsden SC, O'Grady A, Fletcher T, O'Sullivan J, Hart-Holden N, Barton SJ, et al. A clinical molecular genetic service for United Kingdom families with choroideraemia. Eur J Med Genet. 2013;56:432–8.

31. van den Hurk JA, Schwartz M, van Bokhoven H, van de Pol TJ, Bogerd L, Pinckers AJ, et al. Molecular basis of choroideremia (CHM): mutations involving the Rab escort protein-1 (REP-1) gene. Hum Mutat. 1997;9:110–7.

AUTHOR CONTRIBUTIONS
YS participated in study design, data collection and analysis, and manuscript preparation. CC contributed in collecting clinical data of patients, performing molecular experiments analysis, YX, TS, and XK participated in data collection and analysis. YL participated in the study design and revised the manuscript critically for important intellectual content. All authors approved the final version.

COMPETING INTERESTS
The authors declare no competing interests.

ADDITIONAL INFORMATION
Supplementary information The online version contains supplementary material available at https://doi.org/10.1038/s41433-022-01950-6.

Correspondence and requests for materials should be addressed to Yang Li.

Reprints and permission information is available at http://www.nature.com/reprints

Publisher's note Springer Nature remains neutral with regard to jurisdictional claims in published maps and institutional affiliations.